



**UNIVERSITY
OF GÄVLE**

FACULTY OF ENGINEERING AND SUSTAINABLE DEVELOPMENT

Design, Construct and Test of Ultra-Wide Band Triple-
layer Meta-material Absorber

Pu Sun

September 2016

Master's Thesis in Electronics

Master's Program in Electronics/Telecommunications

Examiner: Jose Chilo

Supervisor: Daniel Rönnow

Abstract

In this paper, the design, simulation, fabrication and measurement of an ultra-wideband (UWB) meta-material absorber (MMA) is presented. The proposed MMA is planned to place between transmitter antenna and receiver antenna in a radar detection system in order to reduce the crosstalk. Expected absorption of MMA should be over 90% and covers the frequency band from 1GHz to 4GHz, especially in the frequency bandwidth 2 to 3 GHz which contains most valuable information in the applicate radar detection system.

Since referenced MMAs are resonant absorbers which have typically narrow functional ranges and operate only on single frequency, one has to adjust MMA unit cell's physical parameters to vary its functional frequency bandwidth. But the variation of bandwidth has also its limitation due to the relative frequency theory. Therefore, a triple-layer arrangement design of MMA unit cells is used in this report, in order to generate more variations of physical parameters and gain the flexibility.

Using triple-layer arrangement design on referenced L-shape MMA unit cell, the proposed MMA is simulated using High-Frequency Structural Structure (HFSS), and the fabricated MMA board is measured by vector network analyzer (VNA). In result, simulated absorption bandwidth of the proposed structure is 1.85GHz from 2.25GHz to 4.1GHz, while testing experimental results has 1.5GHz bandwidth from 2.25GHz to 3.75GHz with more than 90% absorptivity.

Table of contents

Abstract.....	ii
Table of contents.....	iv
1 Introduction.....	1
1.1 Thesis Background.....	1
1.2 Problem Statement.....	1
1.3 Aim and Motivation.....	2
1.4 Thesis Outline.....	2
2 Theory.....	3
2.1 What is Meta-Material Absorber.....	3
2.2 Applicate Theory in Designing.....	4
2.2.1 The Key Identification of Absorptivity: Absorption.....	4
2.2.2 Impedance Matching between MMA and Air.....	4
2.2.3 Relationship between Shifting Functional Frequency Band and MMA Scaling.....	6
2.2.4 Relative Frequency Limitation while Scaling.....	7
3 Method.....	8
3.1 Flow Chart of Unit Cell Designing Process.....	8
3.2 L-shaped Meta-Material Absorber.....	9
3.3 Options for Wide-band Absorbers' Unit-cell Arrangement.....	10
3.4 Substrate Material Selecting and Electric Thickness.....	11
3.5 Proposed Meta-Material Absorber Unit cell.....	13
4 Simulation.....	14
4.1 Boundary Condition for HFSS.....	14
4.2 Simulation Results.....	15
4.3 Sensitivity.....	16
4.3.1 Deviation.....	16
4.3.2 Sensitivity on incident angle.....	19
5 Fabrication and Experimental Measurement.....	20

5.1	Fabrication on PCB	20
5.2	Measurement Process	21
5.3	Absorptivity Responses	21
5.4	Absorptivity Results with Variation of Incident Angle θ	23
5.5	Absorptivity Results with Variation of Incident Angle φ	24
6	Conclusion and future work	25
7	Reference	26

1 Introduction

In this section, thesis background, problem statement and motivation of this thesis will be introduced. In addition, the thesis outline is also represented in the end of this section.

1.1 Thesis Background

In 2008, Landy etc. came up with the very first idea of a perfect meta-material absorber, the structure consists of two resonators separately couple to the electric and magnetic fields, so it performs a perfect absorption to incident radiation [1]. In Landy's MMA unit cell design, a FR-4 substrate was placed in between of two copper patches, which one side of them were shaped as a ring-structure electric resonator and the other side was shaped as a cut wire stripe.

Based on his design, researchers after that made many progresses against polarization sensitivity and extend the incident wave angles. For the functional frequency regions, Frequency independent broadband absorbers which can absorb radiation over a wide bandwidth were invented. To overcome the narrow band limit, there are methods such as lump component with absorbers, designing fractal shapes and using frequency selective surfaces (FSS). Consider to the complexity of unit cells' design and the cost of the absorber, using FSS ends up with our best choice in our case.

1.2 Problem Statement

This master thesis project is a collaboration project between Högskolan i Gävle (HIG) and Radarbolaget AB. It is also an extension of university's group project 'Design of Ultra-wide Band absorber in antenna housing made of metamaterial' from course 'Advanced Projects in Electronics 7,5 hp, HT15', which was completed by me and my classmates: Amran Ndolla, Motasim Jameel and Om Parakash Nandi.

Radarbolaget is a radar company providing radar solutions for many applications such as construction and infrastructure, steel and metal industry, energy and paper and process industry. This project was tasked to solve the cross-talk issues between transmitter antenna and receiver antenna in detection and sensing projects, with the digital Ultra-wide band (UWB) radar system which Radarbolaget developed.

In normal circumstances, the transmitter (Tx) and Receiver (Rx) are separated by approximately 20 cm and facing detected objects, and there's always crosstalk in between. For the crosstalk interference, it might be used as reference sometime, but when it's too strong it will create dynamic problems. Normally, to decrease the interference, we can just separate Tx and Rx, but consider to installation restriction under detecting project's situation, we have to find another effective method to decrease the interference. By using an absorber between Tx and Rx, we could get an expected frequency response in specified bandwidth. According to the literature review, meta-material finally has been chosen to be the absorber material because of its high electromagnetic wave absorption capabilities.

1.3 Aim and Motivation

The major objective of this thesis project is to design, construct and test a meta-material absorber which has as better absorptivity as it could be over the frequency region 1GHz to 4GHz. In order to achieve the most effective MMA design in this frequency range, a proper referenced design would firstly be chosen, then a series of optimization and tuning would be done based on it. Finally, the simulated and experimental analysis of determined triple-layer MMA would be given.

1.4 Thesis Outline

This thesis contains three sections, the theory and method parts include the academically theories on designing proposed MMA. Simulation and experimental measurement presents individually the simulated absorption result for MMA on HFSS and the physical measured absorptions. In addition, the measurements parts also attend on the variation of absorptivity results due to the change of incident angles. In the end of thesis, some conclusions and future work of this project is presented as well.

2 Theory

In this section, the history, definition and some key factors of MMA is placed in the first part. Second part is the collection of applicable theories which will be used in designing. It includes absorption's definition which is the key identification of absorptivity, introduction of Fresnel equation which explain the process of matching impedance between structure and free space, which in our case is used to reduce the reflection from the interface. Moreover, it also includes the relationship between physical scaling and frequency shifting, which is developed by mathematical formula. In the end of applicable theories, there's also the relative frequency theory which limits the physical scaling while shifting frequency bandwidth.

2.1 What is Meta-Material Absorber

Meta-materials (MM) are artificial materials that have exotic electromagnetic effect properties which cannot find in nature, they are usually made by combinations of metal and dielectric materials. Their absorptive properties don't come from their base-materials' properties, but the design of its structures. The possibilities to obtain specified reflective indexes, permittivity and permeability, make them applicable to design an absorber. One of the key factors in achieving perfect absorptivity is matching the impedances between air and material, which is theoretically achievable by changing the shapes, orientations, sizes and arrangements of MM structures to obtain the required electromagnetic parameters [2].

In Landy's MMA design, absorber includes an electric resonant ring structure (e-SRR) at front surface and a copper stripe at back. Under the excitation of the incident electromagnetic wave, it can generate electric resonance between the parallel metal structures and generate magnetic resonance in the ring-shaped structure, so that the energy from incident electromagnetic wave is consumed by resonances. The paralleled metal with substrate material in between can be considered as a capacitance while the e-SRR can be considered as an inductance. Therefore, the absorptive frequency region is decided by the circuit which constituted of its equivalent inductor and capacitor. By changing the capacitance and inductance in equivalent circuit, which is corresponding to the MMA's structural parameters, the operating frequency would be changed [3].

2.2 Applicate Theory in Designing

2.2.1 The Key Identification of Absorptivity: Absorption

As we mentioned in section 1.3, the major objective of this thesis project is to design, construct and test a meta-material absorber which has as better absorptivity as it could be over the frequency region 1GHz to 4GHz. But how to determine whether the absorptivity is good enough or not, in this thesis, absorption is used as a key identification of absorptivity.

Absorption $A(\omega)$ of an electromagnetic material is usually introduced by reflection $R(\omega)$ and transmission $T(\omega)$. When electromagnetic wave incident into the MM Structure, the absorption could be calculated as Eq1 and Eq2 below:

$$A(\omega) = 1 - |R(\omega)|^2 - |T(\omega)|^2 \quad (1)$$

Or

$$A(\omega) = 1 - |S_{11}|^2 - |S_{21}|^2 \quad (2)$$

In many cases, when there is a copper back at the end of a structure, then the absorption comes to

$$A(\omega) = 1 - |S_{11}|^2 \quad (3)$$

It means the value of absorption is only decided by the reflection $R(\omega)$ while $R(\omega)$ is decided by the impedance of absorber-surface's equivalent wave.

Also, it should be noted that, for S_{11} value less than -10 dB corresponding to 90% of the absorption of the incident wave.

2.2.2 Impedance Matching between MMA and Air

One of the key factors in achieving perfect absorptivity is matching the impedances between air and material, as we mentioned in 2.1 above. As a mathematical tool to describe the behavior when an electric-magnetic wave propagates through two different media, Fresnel equation can be used in MMA cases to describe the impedance matching condition between MMA and air.

From the equation, in using of the reflection index for both media, which part of fraction of incident wave is reflected and which part of fraction is reflected could be found. Consider the MMA itself has a thickness of d , and it can be described by both the magnetic permeability $\mu(\omega) = \mu_0\mu_r(\omega)$ and the electric permittivity $\varepsilon(\omega) = \varepsilon_0\varepsilon_r(\omega)$. At the back side of the substrate, there's a back metallic plate with high conductivity (structure of our referenced MMA unit cell design, which has a clear description in section 3.1). So, for transverses electric (TE) and transverses magnetic (TM) polarized wave, by considering the reflectivity (R) and reflection coefficient (r) of an interface [4], we can get Eq4 and Eq5 as below:

$$R_{TE} = |r_{TE}|^2 = \left| \frac{\cos \theta - \mu_r^{-1} \sqrt{n^2 - \sin^2 \theta}}{\cos \theta + \mu_r^{-1} \sqrt{n^2 - \sin^2 \theta}} \right|^2 \quad (4)$$

$$R_{TM} = |r_{TM}|^2 = \left| \frac{\varepsilon_r \cos \theta - \sqrt{n^2 - \sin^2 \theta}}{\varepsilon_r \cos \theta + \sqrt{n^2 - \sin^2 \theta}} \right|^2 \quad (5)$$

Where, in the equations, θ is the incident angle, $n = \sqrt{\mu_r \varepsilon_r}$ is the MMA's refraction index.

If we constrict the incident wave to normal, as make θ equals to zero, Eq4 and Eq5 reduce to:

$$R = \left| \frac{Z - Z_0}{Z + Z_0} \right|^2 = \left| \frac{\mu_r - n}{\mu_r + n} \right|^2 \quad (6)$$

Where $Z = \sqrt{\mu/\varepsilon}$ is the impedance of the MMA material and $Z_0 = \sqrt{\mu_0/\varepsilon_0}$ is the impedance of free space.

Since we considered a metallic plate is placed at back, from chapter 2.2 Eq1 we can have our absorptivity as:

$$A = 1 - R = 1 - \left| \frac{Z - Z_0}{Z + Z_0} \right|^2 = 1 - \left| \frac{\mu_r - n}{\mu_r + n} \right|^2 \quad (7)$$

From Eq7 above, it can be found out that the perfect matching between MMA and air could be reached by adjusting the value of relative permeability and refraction index of MMA. The difference between relative permeability and refraction index can reflect the impedance difference between air and MMA.

2.2.3 Relationship between Shifting Functional Frequency Band and MMA Scaling

For MMAs, different sizes of resonant ring structures are corresponding to different functional frequencies. To shift the functional frequency bands from high frequency to low frequency or the way inverse, one has to firstly figure out the relationship between size scaling and frequencies.

Due to the theory of MMA, the functional frequency's wavelength is tightly corresponding to the dimensions of MMA, the ratio between them can be considered as a constant. Therefore, the relationship between MMA dimensions and bandwidth can be transferred to the relationship between related wavelength and functional frequency bandwidth. The relationship between frequency of the electromagnetic wave and its wavelength comes from the Eq8:

$$c = \lambda f \quad (8)$$

Consider two frequencies which has relationship $\lambda_1 = a\lambda_2$, where a is a constant. We have:

$$c = \lambda_1 f_1 \quad \text{and} \quad c = \lambda_2 f_2 \quad (9)$$

The speed of light (c) could not be changed in the vacuums, so we have

$$\lambda_1 f_1 = \lambda_2 f_2, \text{ since } \lambda_1 = a\lambda_2, \text{ then we have } f_1 = \frac{f_2}{a} \quad (10)$$

Now, it's clear that the wavelength and relative frequency value is linearly related. In order to obtain our frequency range (1GHz to 4GHz), from the original L-shaped MMA unit cell we introduced in chapter 3.1 which has frequency response from 4.6GHz to 7.2GHz. The size of structure should be decreased by from 4.6 times (4.6GHz divides by 1GHz) to 1.8 times (7.2GHz divides by 4GHz).

2.2.4 Relative Frequency Limitation while Scaling

While shifting functional frequency bandwidth from referenced design to the expected range by scaling the dimensions of structure, the bandwidth variations due to relative frequency has to be noticed. Consider of a bandwidth in higher frequency from f_{start} to f_{end} , has a bandwidth of B_w as Eq11 below

$$B_w = f_{end} - f_{start} \quad (11)$$

While shifting B_w to lower frequency range by extending dimensions by a times, which the related wavelength is also extended by a. Combine Eq10 and Eq11, the bandwidth after shifting can be expressed as Eq12 below.

$$B'_w = f'_{end} - f'_{start} = \frac{f_{end}}{a} - \frac{f_{start}}{a} = \frac{B_w}{a} \quad (12)$$

The length of the bandwidth is therefore inversely proportional to MMA's physical dimensions. When the physical dimensions extend by a time, the shifted bandwidth is 1/a times compressed compare with original bandwidth.

For example, our referenced L-shape MMA design originally has a functional frequency bandwidth of 2.6GHz from 4.6GHz to 7.2GHz, once we increase the physical dimensions and shift it to our expected frequency range (1 - 4 GHz). Assume the shifted bandwidth starts from 2GHz, then it will end at 3.1GHz and the bandwidth is compressed from 2.6GHz to 1.1GHz. In conclusion, the expected UWB frequency response couldn't easily achieved by just change the dimensions of referenced MMA, more improvement on orientation, arrangement or ratios among exist physical parameters have to be done in order to approach our aim.

3 Method

In this section, the method using to design MMA's unit cell is discussed. Firstly, the flow chart of the designing process is introduced. In the flow chart, the L-shaped referenced unit cell, triple-layer arrangement and substrate material ISO680 is considered as fixed input, the reason why they have been selected and all considerations about them are discussed individually after the flow chart section. Lastly, the output proposed unit cell structure using this methodology is presented.

3.1 Flow Chart of Unit Cell Designing Process

The flow chart of unit cell's designing process is presented as Fig1 below. In the process, L-shaped reference unit cell, triple-layer unit cell's arrangement and substrate material: ISO680 are considered as three initial input. This is because of the determination came from literature review and other considerations which are limited in this project.

In the adjustment process, the physical parameters include three basic L-shaped parameters 'l', 'w' and 'd' in each layer (more details on section 3.2), as well as the substrate thickness between L-shaped layers or between L-shaped layer and back copper plate.

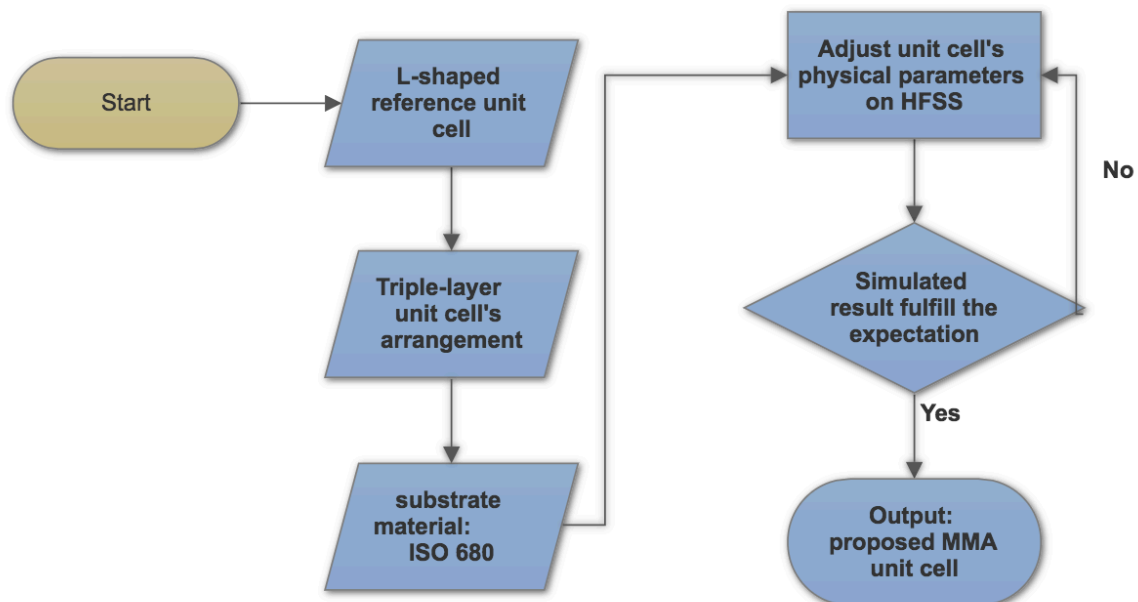


Figure 1 Flow chart of unit cell's designing process

3.2 L-shaped Meta-Material Absorber

The design of triple layer MMA of this paper is originally referenced by L-shaped patched from ‘A Broadband Wide Angle Meta-material Absorber for Defense Applications’ [5]. On the paper, a single layer structure is presented, while L-shaped patches placed at the top surface while a copper plate on the back. This absorber has an absorption bandwidth which is over 90% absorptivity from 4.6 to 7.2 GHz. The front view of the unit cell is as shown as Fig2 below, which is modeled as a square, two L-shape copper film are geometrically symmetry at the surface. The incident electromagnetic wave direction, electric field and magnetic field direction are determined by arrow ‘k’, ‘E’ and ‘H’.

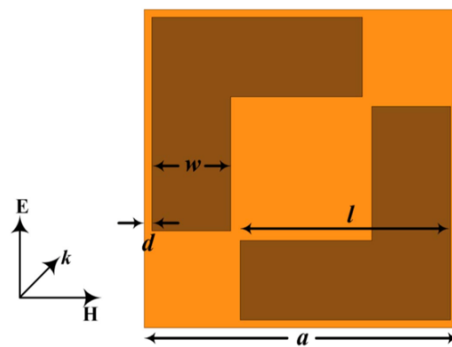


Figure 2 The L-shaped unit-cell from Ref [5], with incident direction 'k', E-field direction 'E' and magnetic field direction 'H'.

In the design, they used four parameters to model the surface design of unit cell. ‘a’ is the side length of the square which mainly decided the size of unit cell which is also the size for the back copper plate. ‘l’, ‘w’ and ‘d’ are using to describe the size of L shape, which stand separately for length of the L-shaped bar, width of the L-shaped bar and the gap distance between L-shaped bar to the edge of unit cell. Furthermore, the thickness of copper and the thickness of substrate between the top surface L-shaped copper film and back copper plate have also influence on the functional frequency bandwidth.

The original design from the reference paper, which has more than 90% absorptivity from 4.6 to 7.2GHz, has $a = 10mm$, $w = 2.5mm$, $d = 0.25mm$, $l = 6.7mm$ as its value. The triple layer design is based on these parameters and followed the rules for scaling to shift the functional frequency bandwidth to our expectation region.

3.3 Options for Wide-band Absorbers' Unit-cell Arrangement

With the development of meta-material researches, scientists came up many methods to overcome the operating frequency's narrow-band limitation. Here's a quick overlook for three most effective ways to approach.

First attempt was made in Tao's [6] design, a composite SRR structure is combined by two SRRs with different sizes. Because of functional frequencies are related to different sizes of frequencies (in chapter 2.3.2), two resonant rings in his design relates individually on 1.4 THz and 2.9 THz, which has 86% and 84% absorptivity. They combined geometrically, arrange them as that their split resonant ring's share a common bar, then two operating point can be observed. The combined structure can operate same time at 1.4THz and 2.9THz. In the combined structure, the larger size resonator is corresponding to low-frequency response while the small size corresponds to the higher frequency response due to the surface current analysis.

Another selected method is given by Luo [7], He came up with a solution with five different-scaled SRRs arrange in a co-planar. The composite structure is shown as Fig 3 below, the dimensions of these five individual unit cells are scaled up from left to right, and the relative frequencies are individually from 9 to 12GHz.

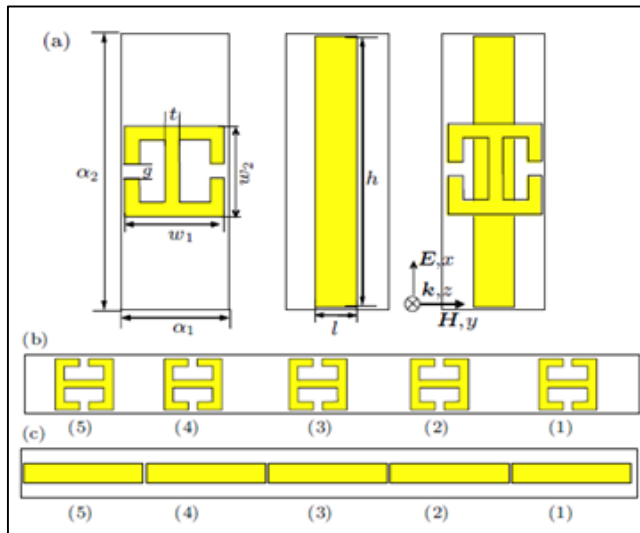


Figure 3 Arrangement for Luo's[8] design

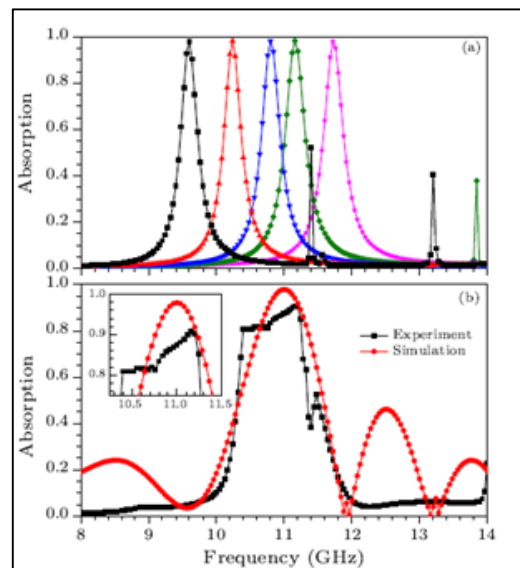


Figure 4 Simulated and experimental result for Luo's [8] design

The frequency response for the combined structure have five frequency responses (as Fig4 last page) combined tightly as a wide-band absorption which has 1.3GHz bandwidth from 10.4GHz to 11.7 GHz. It is done to achieve the peaks to overlap with one another, which will result a wide band operation.

At last, there's another method with putting SRR and substrate structures layer by layer. Sun [8] has a successful design for it, he designed the physical parameters for MMA unit cells to let each layer have specified infraction index, in order to offset the incident electromagnetic wave with reflected wave. To put three different sized resonant rings layer by layer as well as a coper patch on behind, His multi-layered MMA design achieved such simulation results: the absorber has a more than -10dB's absorption between 5GHz to 30GHz, and a very strong absorption around 20GHz.

Among the three methods above, the multi-layer MMA designed has been selected in our project since its high potential to obtain broadband absorptions. Compared with other two methods, it overcame the disadvantage of narrow band absorption. Even though the designed arrangement or combination of SRRs can expand the absorptive bandwidth, but it has limitations for that and has to trade off with the size of the whole absorber [9].

3.4 Substrate Material Selecting and Electric Thickness

By creating a multi-layer MMA, the thickness of the entire absorber has to be considered as a key feature. For reducing the thickness, a feasible method is to change the material of the substrate. Consider the situation when plan waves propagate through a lossless medium, the velocity of the propagating wave is called phase velocity because it is the velocity at which a fixed phase point on the wave travels [10], and it is given by

$$v_p = \frac{dz}{dt} = \frac{d}{dt} \left(\frac{\omega t - \text{constant}}{k} \right) = \frac{\omega}{k} = \frac{1}{\sqrt{\mu\epsilon}} \quad (13)$$

Where $k = \omega\sqrt{\mu\epsilon}$ is defined and called propagation constant (also known as the phase constant, or wave number), of the medium, its unit are 1/m [10].

Combined with Eq8 on page 5, we have:

$$\lambda = \frac{c}{f} = \frac{\frac{1}{\sqrt{\epsilon}}}{f} = \frac{1}{f\sqrt{\epsilon}} \quad (14)$$

So the wavelength inside the medium has linear relationship with $1/\sqrt{\epsilon}$. If we definite d as physical thickness for the substrates, then we can definite electric thickness as:

$$d_e = d/\sqrt{\epsilon} \quad (15)$$

Then we can decrease the thickness of substrate as well as keep the absorptive properties by finding the proper material with specified dielectric loss parameter due to Eq15. As an example, in this project, a new substrate material has been recommended by Radabolaget AB. The key features for this material ISO680-345 is shown as table 1 below.

Table 1 Key features for ISO680-345

<p>ISO 680-345 Data Sheet</p> <p>Tg 200, Td 360 Dk 3.45, Df 0.035 /17</p>
<p>Features</p> <ul style="list-style-type: none"> • High Thermal Performance <ul style="list-style-type: none"> ❖ Tg:200°C(DSC) ❖ Td:360°C(TGA@5%wt loss) ❖ Low CTE in the Z-axis – 2.9% (-55-288°C) • T260:60+ minutes • T288:60+ minutes • RoHS Compliant • Electrical Properties <ul style="list-style-type: none"> ❖ Dk: 3.45±0.05 ❖ Df: 0,0035±0.0005 ❖ Exceptional dielectric properties over a broad frequency and temperature range per IPC-TM-650-2.5.5.5

For ϵ value of this material, compared with the one with FR-4 which is equal to 4.4, in conditions of having the same electric thickness, the physical thickness is calculated (as eq.15 below) as 0.885 times thicker than FR-4 ones, the calculation is given by Eq16 below

$$d_{ISO680} = \frac{\sqrt{3.45}}{\sqrt{4.4}} d_{FR-4} = 0.885 d_{FR-4} \quad (16)$$

3.5 Proposed Meta-Material Absorber Unit cell

By using the same L-shaped model in Fig2 on page 9, the triple-layer has its physical parameters as shown in table 2 as below:

Table 2 Parameters for proposed MMA unit cell

	L (length)	W(width)	d (distance to edge)	T_s (thickness of substrate)
Top Layer SRR	10.5mm	1.5mm	1.8mm	2.28 (1.52+0.76) mm
Middle Layer SRR	11.25mm	1.5mm	1.05mm	2.28 (1.52+0.76) mm
Down Layer SRR	6.03mm	2.25mm	0.45mm	4.56 (3*1.52) mm
a (Side length of unit cell) : 18 mm			T_c (thickness of copper film): 0.035 mm	

The thickness of substrates is limited by the two optional thickness of ISO680 slabs in this project, the thickness should be 0.76mm, 1.52mm or any combinational additions of these two values. For using the parameters in Table.2, the outlook of proposed MMA unit cell is plotted using ANSYS High Frequency Structural Simulator (HFSS) as shown Fig5 below.

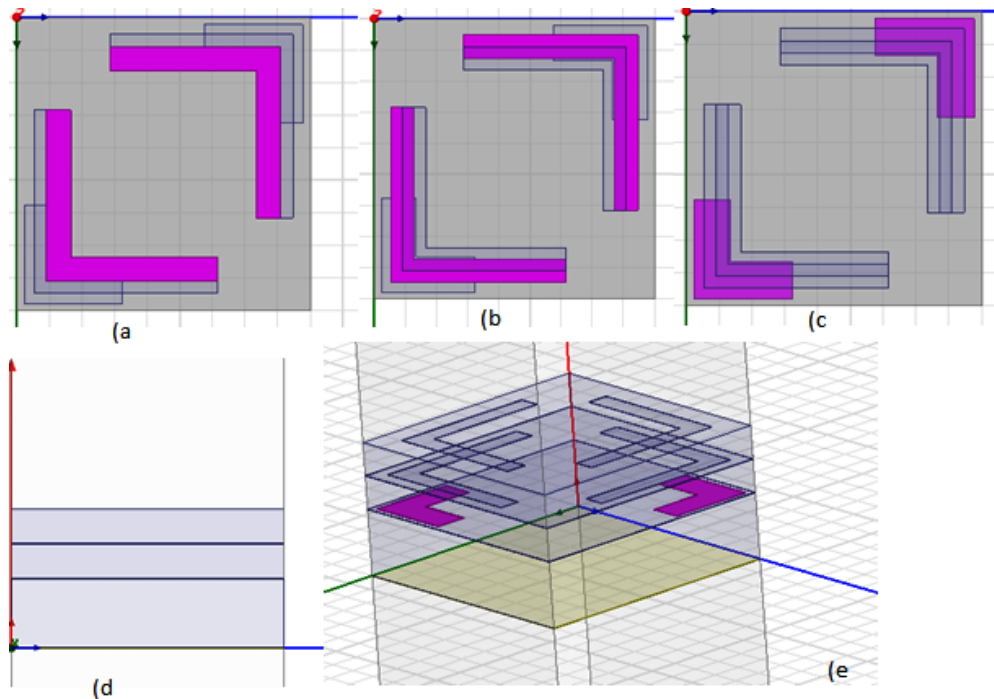


Figure 5 Overview for proposed MMA unit cell a) top layer b) middle layer c) down layer d) side view of thickness e) 3-D view of entire structure

4 Simulation

In this section, the simulation steps use to simulate the proposed MMA's unit cell using software High Frequency Electromagnetic Field Simulator (HFSS) are introduced. Firstly, the boundary condition setups in the software is represented, which is the most important setup in simulation. Then the result and discussion about them are studied. At last, the sensitivity test of the structure which includes deviation test and sensitivity test on incident angles are presented.

4.1 Boundary Condition for HFSS

For the boundary conditions, we are using Master/Slave conditions which are also called the Linked Boundary Condition (LBC) from HFSS. This combination is widely using to model periodic structures or large repeating, such as infinite antenna arrays or frequency selective surfaces (FSS). LCB includes two types of boundaries which are master boundary and slave boundary, they appear simultaneously all the time. In addition, the shape, size and direction of them must be exactly same. The electric field on master boundary surface and slave boundary surface, they have some phase difference, which is the phase difference between neighboring cells in periodic structures [11].

Assume the distance between master and slave boundary surface is d/λ , electromagnetic wave propagation direction has respectively angle φ and θ with x-axis and z-axis. Then the E-field on master boundary surface has the relation with E-field on slave boundary surface as equation (17) shows below:

$$E_{slave} = e^{j\Phi} E_{master} = e^{j\frac{d}{\lambda} \sin\theta \cos\varphi} E_{master} \quad (17)$$

In the equation, phi is the phase difference between master and slave boundary surface, and has:

$$\Phi = \frac{d}{\lambda} \sin\theta \cos\varphi \quad (18)$$

While defining the master and slave boundary condition, one can definite directly the phase difference between master and slave boundary surface, or definite the scanning angle φ and θ and let the software compute the phase difference instead.

When using a pair of this combination in simulating, the slave surface is forced to match the E-field on another, the master surface, to within a phase difference [11]. For simulation port excitation, it's reliable to use the Floquet port. Together with Master/Slave boundaries, they can create an accuracy environment for simulation.

4.2 Simulation Results

By simulating the MMA unit cell model, set two pairs of master/slave boundaries around it and Floquet ports on both front and back side, create enough space between Floquet port and MMA surface, and then run the simulation, we can get the stable simulated result as Fig6 shown below.

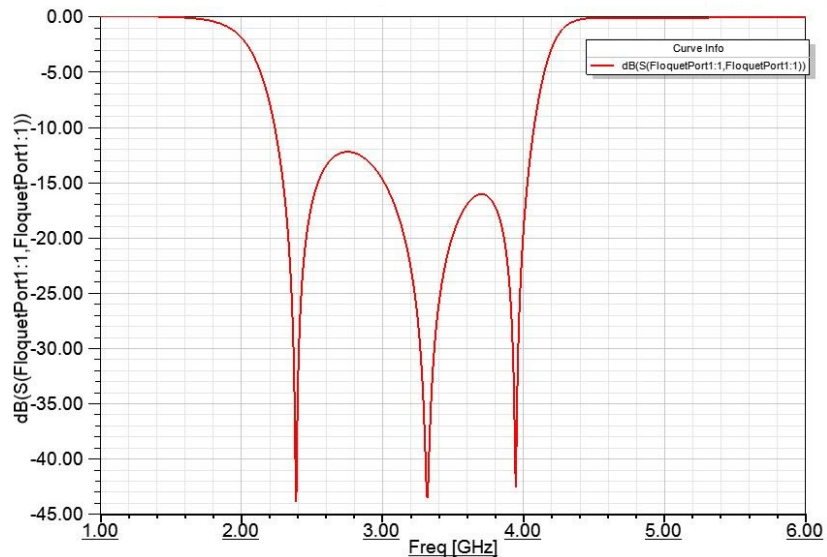


Figure 6 S11 response for MMA with normal incident angle

From the figure, the S_{11} value is lower than -10dB from 2.2GHz to 4.1GHz, which means we have 1.9GHz absorptive bandwidth which has more than 90% absorptivity. By inputting the equation of absorptivity, the plotting of absorption due to the same simulation process could be generated, as shown in Fig7 below.

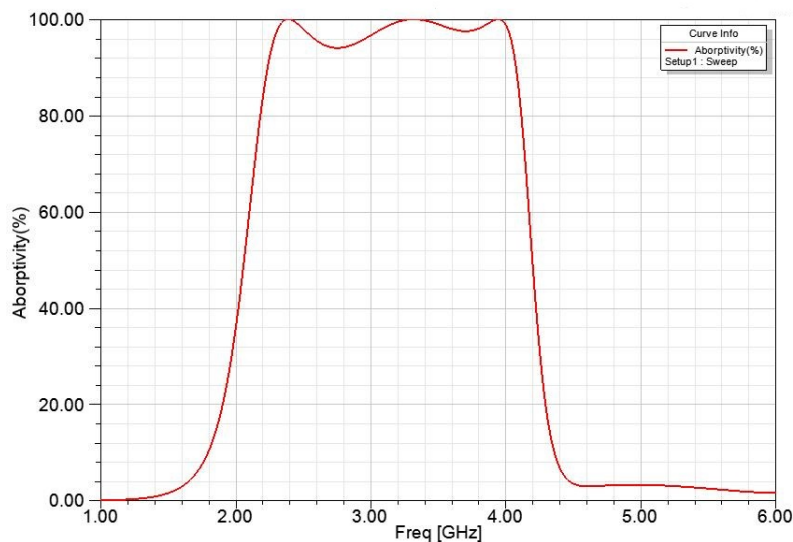


Figure 7 Absorptivity plotting for MMA with normal incident angle

4.3 Sensitivity

In this section of thesis, the sensitivity of simulated MMA will be tested. The sensitivity is defined into two parts here, which is deviation and sensitivity on incident angle.

In deviation part, the parameters among length, width and thickness of MMA will be varied, in order to figure out how sensitive the MMA is relied on these parameters. Reflect to reality, it could not only help with analyzing the error due to inaccuracy manufacturing, but also give an idea on how to shift the operating frequencies.

In the second part, the incident wave θ and φ will be changed in the slave boundary condition setting options. This simulation will test the sensitivity of polarization for the proposed MMA design.

4.3.1 Deviation

For multi-layer structures, it's really complicated to find the consequences from parameter changes to frequency shift, since it has a complex system inside. In order to get an idea how these parameters related to frequency responses, Table3 below is designed. It states up the changing of frequency responses due to variations of length, width, distance to edge and substrates thickness parameters on the top layer. In order to compare the frequency response with different physical parameters, four statuses for each parameter are designed, which are original value, one step decreased, one step increased and two steps increased. The size of steps for each parameter is designed separately, so the variation on frequency can be detected easily.

Table 3 Frequency responses due to varied physical parameters on top layer

Parameter	One step decreased		Original value		One step increased		Two steps increased		Size of step
	Start (GHz)	End (GHz)	Start (GHz)	End (GHz)	Start (GHz)	End (GHz)	Start (GHz)	End (GHz)	
Length	2.2	4.1	2.2	4.1	2.2	4.05	2.2	3.95	2%
Width	2.15	3.9	2.2	4.1	2.45	4	2.2	4.05	33.3%
Distance to edge	2.17	4.07	2.2	4.1	2.23	4.13	2.26	4.18	22.2%
Substrate Thickness	2.3	4.15	2.2	4.1	2.16	4.05	2.1	3.9	21.9%

Compare with the results in Table2, for length parameter, the frequency response doesn't change when it decreases by 2%. But when length parameter increases by 2%, the frequency bandwidth compresses 0.05GHz from the high frequency side, which is corresponded to 2.6% of the whole bandwidth. When length keeps increasing by 4%, the high-frequency side of bandwidth is kept compressing by 0.5GHz. In conclusion, the changes on length parameter could result in the compression of bandwidth. In low frequency range, the bandwidth will keep its value but will decrease in the high-frequency range. A 2% level of change around original value on length parameter could cause a 2.6% level of compression in frequency bandwidth result.

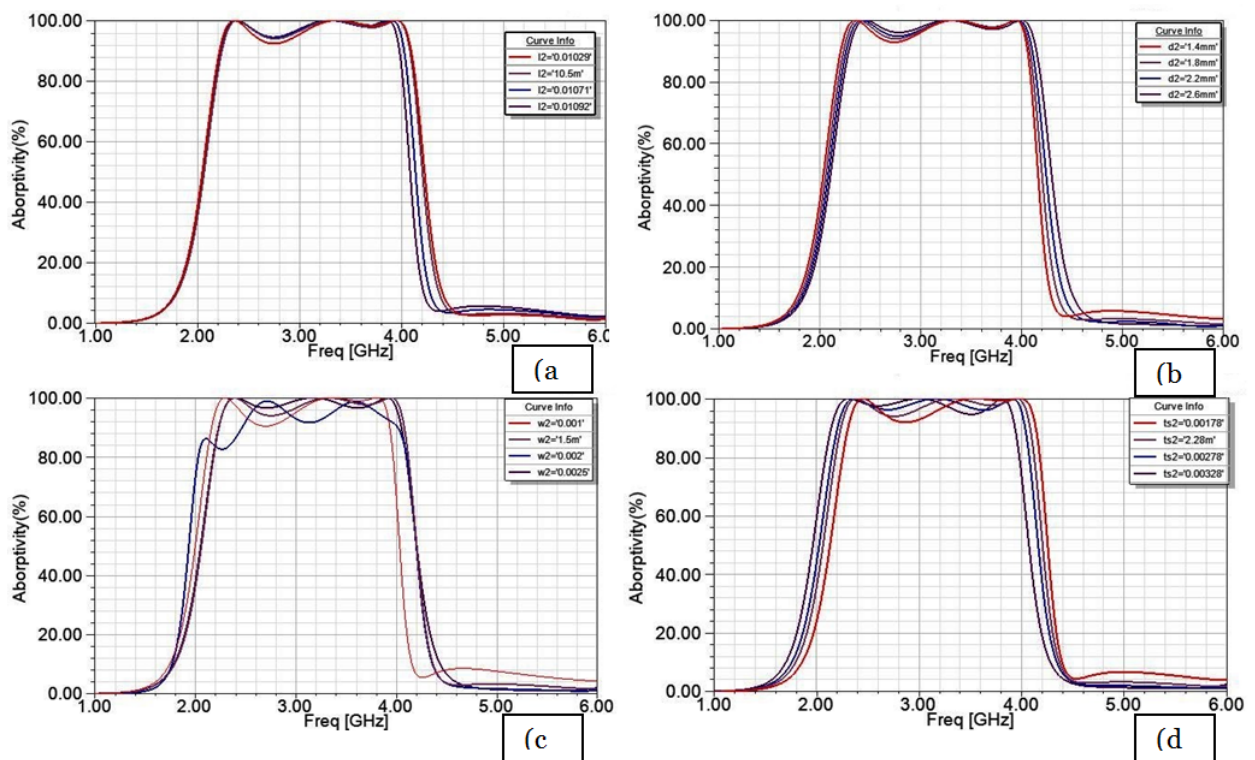


Figure 8 changing of frequency responses due to variations of (a) length parameter 'l' (b) distance to edge parameter 'd' (c) width parameter 'w' (d) substrate thickness parameter 'ts'

For distance to edge parameter 'd', with decreasing or increasing it by 22.2%, the bandwidth will keep its value and moving from low frequency side to high frequency side by a step of 0.03GHz (1.6% of the whole bandwidth). When increase it by 44.4%, the bandwidth will keep moving to high-frequency side, but due to the relative frequency theory, the value of bandwidth increases from 1.9GHz to 1.92GHz. So, for variation of distance to edge parameter, a level of 1.6% of whole bandwidth's shifting will be made by changing the parameter by 22.2% around its original value.

For width parameter, the original width is 1.5mm, and by varying it from 1mm to 2.5mm with a step of 0.5mm (33.3% of original width), both the absorption and frequency response have been changed. When decreasing the width, the frequency response shifted to left, and due to the relative frequency theory, the bandwidth is also decreased from 1.9GHz to 1.75GHz. And with increasing 33.3% of width parameter, the effective bandwidth (more than 90% absorption) is decreased from 1.9GHz to 1.55GHz. It happens because of the absorptivity level is affected by the changing. If consider to the bandwidth from 80% absorptivity, the bandwidth of 33.3% increased width is expanded 0.2GHz in the low-frequency side. When width parameter increases by 66.7%, the effective bandwidth decreases 0.05GHz in high-frequency side because of the decreasing of absorptivity.

For width parameter, the changing of parameter has stronger effect on changing the absorptivity rather than shifting the bandwidth. Consider only the effect on shifting, by changing width parameter around original value with a level of 33.3%, a 0.15GHz (7.9%) level of shifting will happen on bandwidth towards the low-frequency side.

The thickness parameter's result is quite similar to distance parameter, but in the way reverse. With increasing of thickness, the frequency response shifts towards the lower frequency side. Each step is around 0.05GHz which is corresponding to 2.6% of the entire bandwidth. The step of thickness parameter's changing is equal to 21.9%.

In conclusion, compare with changing of these four physical parameters, width parameter has the strongest effect on influencing the absorptivity. Consider to the bandwidth shifting, the length parameter is most effective on influencing it. By changing 2% of its value around the original design, it causes a shifting of frequency response by 2.6% of the whole bandwidth, which we need to change 21.9% of substrate's thickness to archive the same effect.

Reflecting the results to manufacturing processes, a high-quality drifting machine is required. Because even a 0.2mm deviation on length parameter would cause a frequency response shifts by 2.6% of its entire bandwidth.

4.3.2 Sensitivity on incident angle

By changing the phi and theta values in the phase delay setting under slave boundary condition setting on HFSS, the frequency responses rely on different scan angle can be plotted as Fig9 shows as below.

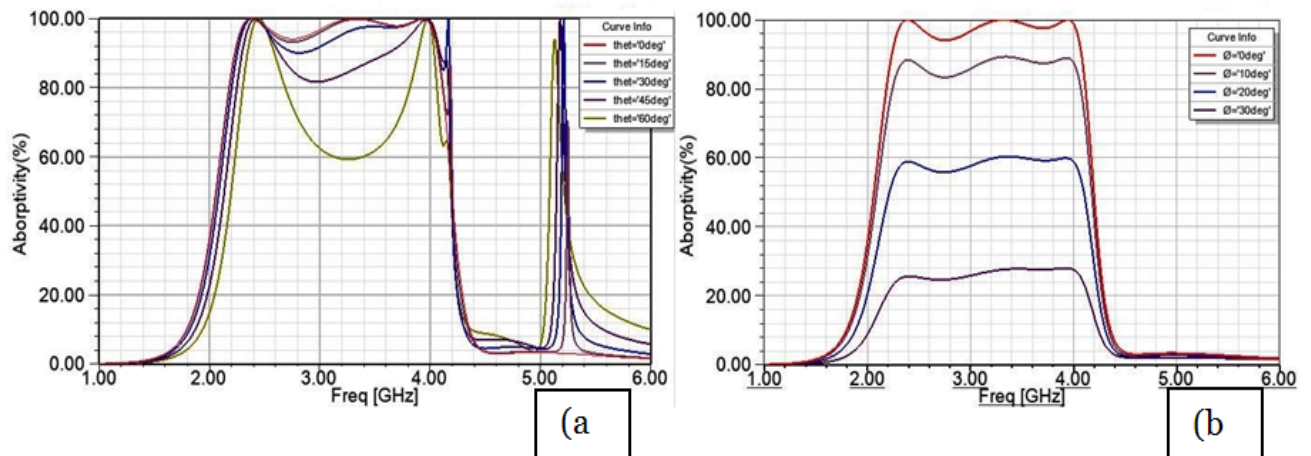


Figure 9 Frequency change due to (a) variation of incident angle parameter ' θ ' (b) variation of incident angle parameter ' ϕ '

In Fig12 (b), the absorptivity varies a lot with change of scan angle phi, the average absorptivity in the operating bandwidth decreases from average 95% to 86%, then 60% until 25%, where the phi value is increasing from 0 to 30 degrees. However, the bandwidth of the operating frequency is stable in this case, it doesn't vary that much compare to the behavior of absorptivity, and it goes down from 1.8GHz to 1.6GHz.

In Fig8 (a), the changing of absorptivity due to variation of scan angle theta is shown. Compare with the response with phi-changing on the right, the operating bandwidth keeps with the changing of theta scan angle, the only thing changed in this case is the absorptive behavior inside the operating bandwidth, as it can be seen from figure, with increasing of theta angle, the absorptivity at 3.2GHz, which is a center frequency point inside the entire operating bandwidth, is changed from 100% to 60%.

5 Fabrication and Experimental Measurement

After obtained expected result from software simulation, the design is fabricated as a printed circuit board (PCB). In this section, the fabrication process, measurement process and experimental results on fabricated PCB is discussed. Likely to the simulated sensitivity test on different incident angles, the experimental ones are also discussed under different variation of incident angle θ and ϕ in the end of this section.

5.1 Fabrication on PCB

PCB stands for printed circuit board, it mechanically supports and electrically connects electronic components using conductive tracks, pads and other features etched from copper sheets laminated onto a non-conductive substrate [12]. In our case, the proposed design was exported to Gerber file, and been sent to a manufacturing factory.

After one and half month, we got our MMA samples in 30cm*30cm scales as shown in Fig10 below. One Swedish crown's coin has been used for scaling in these graphs. The size of the MMA board is 30cm*30cm, there are 15*15 unit cells and the gap distance between edges the nearest unit cell beside it is 1.5 cm.

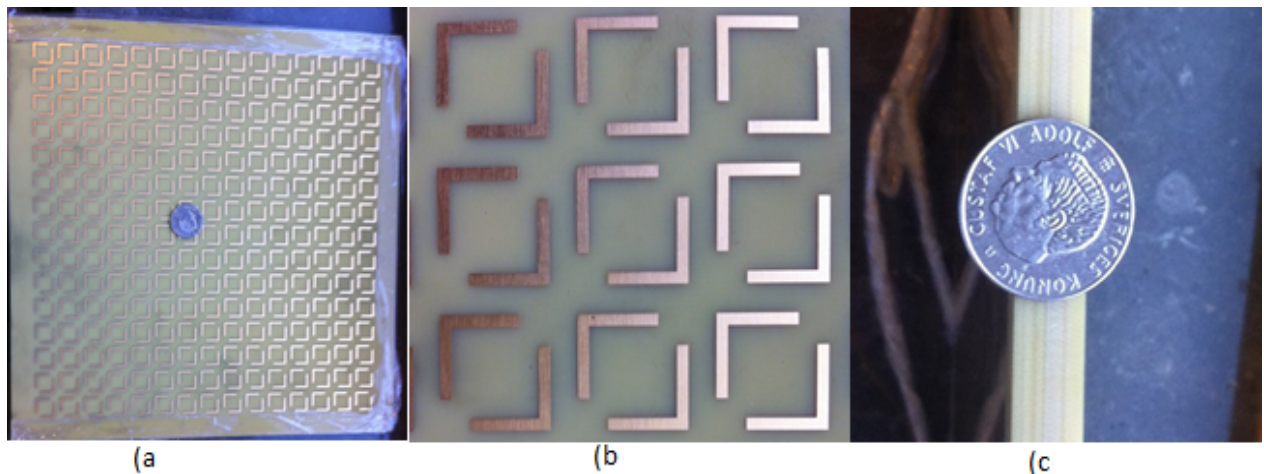


Figure 10 manufactured PCB board a) entire MMA PCB, b) details with 3*3 MMA arrays, c) thickness of substrate comparing with 1 SEK coin

5.2 Measurement Process

The whole measurement process was done in the electric lab room at HiG. For testing the absorption of our manufactured MMA board, two horn antenna, and a chamber. Inside the electric chamber, PCB is hanged in one side, two horn antennas place one the other side, one is used as transmitter while another is used as receiver, two antennas face the PCB with same angle.

The metallic surface side of MMA is firstly being measured as a reference of full reflection data, then the MMA structured side is tested as well. The ratio between it and the reference is considered as the absorptivity of MMA. For testing the absorptive response with oblique incident angles, the hybrid standers for the horn antenna are used to adjust the angles for both theta and phi.

5.3 Absorptivity Responses

The reading from VNA for the normal incident direction case is shown as Fig11 as below. From the figure, the red line presents the full reflection which is measured by putting horn antennas facing the metallic side of MMA board. The green line is the frequency responses for the MMA structured side of board, the ratio of two trace is calculated by VNA, and shows as the blue trace in the figure.

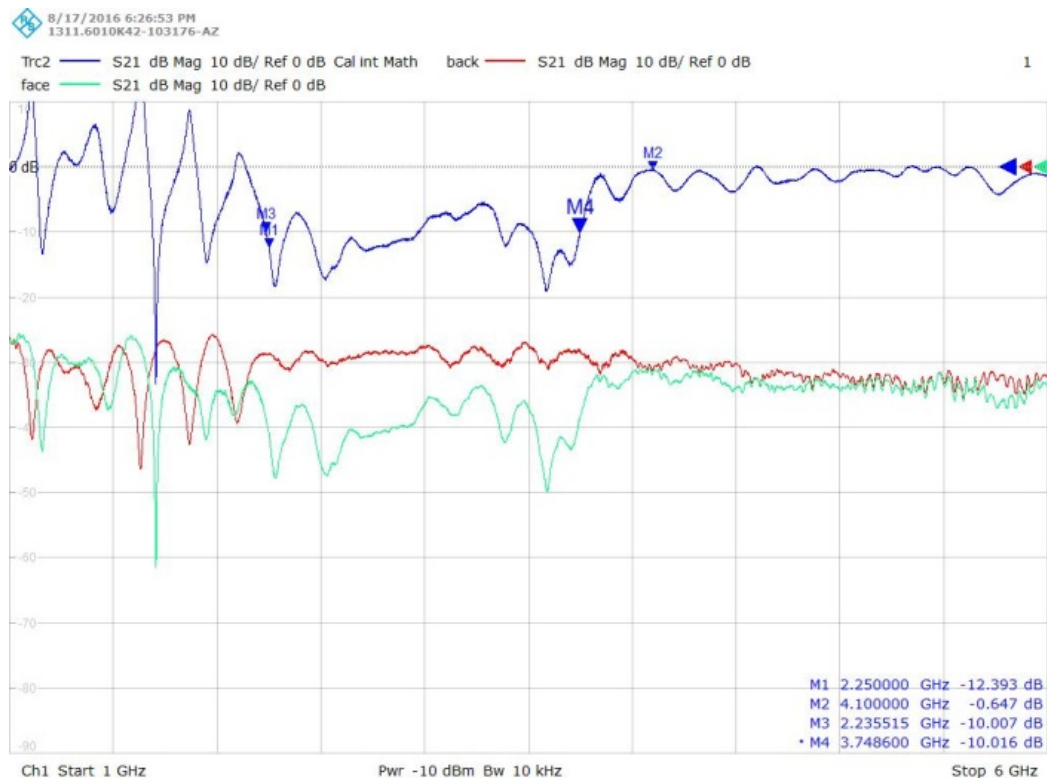


Figure 11 the reading on VNA while testing normal incident wave

In Fig11, four markers present the expected bandwidth values and the operating frequency band in reality. The tested functional frequency band is from 2.24GHz to 3.75GHz. Compared to designed value which is from 2.25GHz to 4.1 GHz, the experimental result accomplishes 80% of the bandwidth goal.

By exporting the measured data from VNA and plotting with MATLAB software, we can get the comparison between simulated result from HFSS and experimental result from VNA. The plotting for normal incident direction case is shown as Fig12 below.

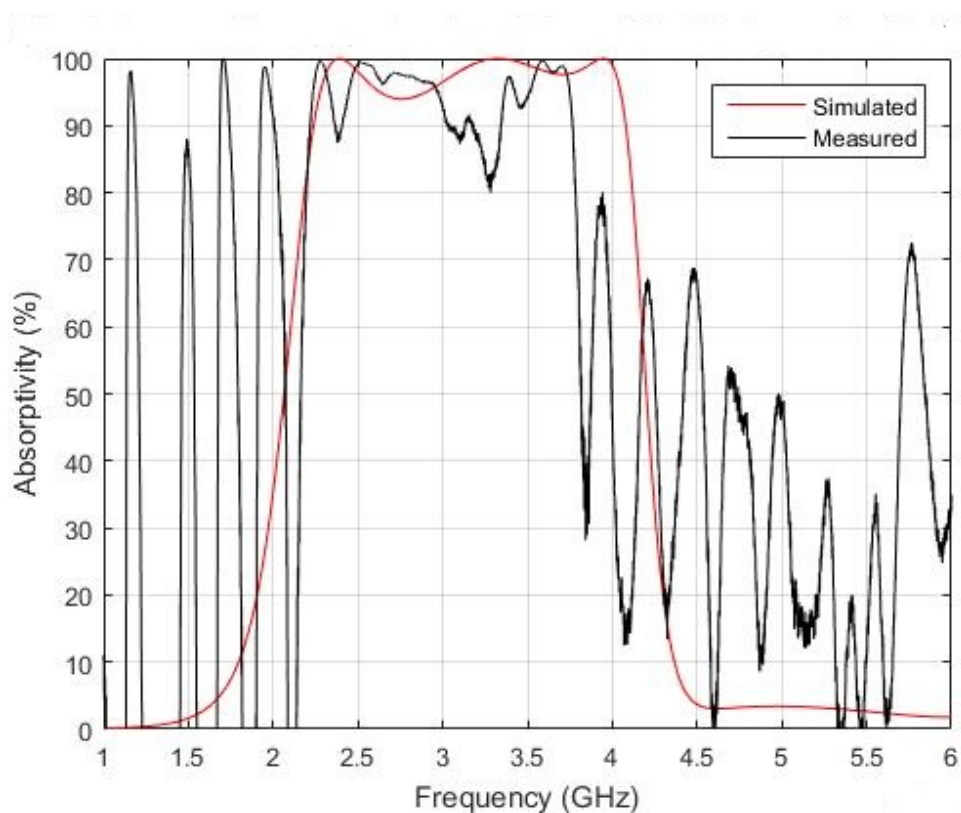


Figure 12 Experimental results versus simulated result in normal incident wave condition

From Fig12, as same as it can be seen from S11 reading on VNA, the manufactured MMA board has 80% bandwidth than we expected, which is from 2.25GHz to 3.75GHz. Something should be noticed is the frequency behaviors before 2GHz. The flexible frequency responses under low frequency ranges, they are caused by the MMA board edge effect. Since the size of MMA board (30cm*30cm) is limited, the frequency response is not reliable for the electromagnetic waves with long wavelengths compared with the board size.

5.4 Absorptivity Results with Variation of Incident Angle θ

In order to test the sensitivity of MMA with oblique incident angles, the incident direction of horn antennas have been adjusted with specified angles, the experimental results for frequency responses compared with simulated result which have already presented in chapter 4.3.2.

The experimental results for absorptivity in different angles are plotted Fig13 below. Compare with Fig9 (a, if we ignore the instabilities in experimental testing, which consider these instable peaks in low and high frequency ranges are a smooth line through its average values, we could find the experimental result has the same absorptivity behavior as simulated result. From Fig13, up to 45 degrees, the absorptivity results have more than 80% in average. Once it increases to 60 degrees, the absorptivity loses its stability and varies a lot inside bandwidth.

Compare with simulated result, the tested results have almost same size of bandwidth but shift approximately 300MHz in average to the low-frequency side. Due to the limitation of the experimental environment, that doesn't have enough space inside the electric chamber. The variation of theta can not be adjusted very accuracy, especially between 45 degrees to 60 degrees where the horn antennas are too close to the edge. But according to the further testing, until 50 degrees of theta angle, the frequency result has a stable response inside its bandwidth.

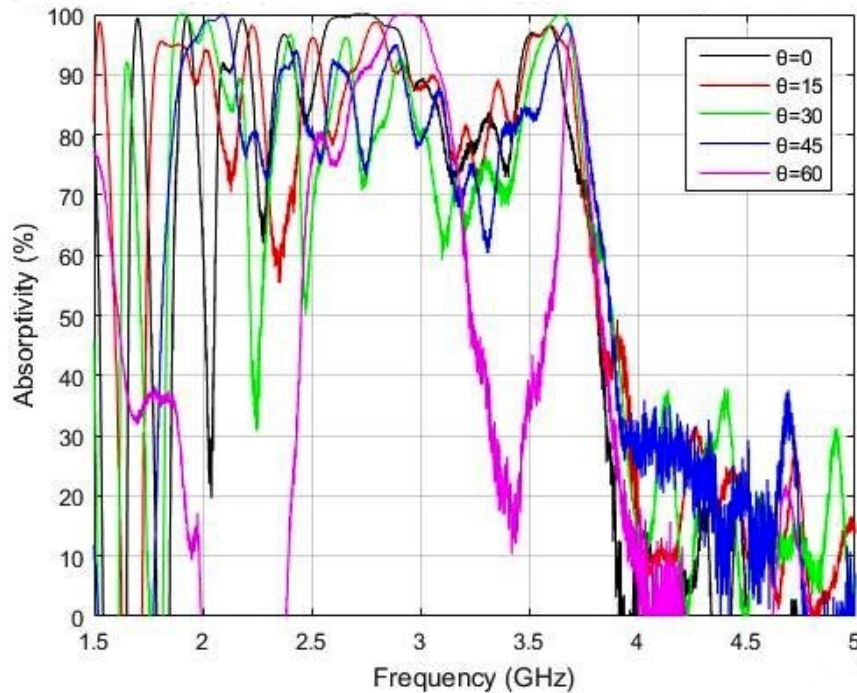


Figure 13 Absorptivity versus Frequency responses from oblique incident angle from 0 up to 60 degree

5.5 Absorptivity Results with Variation of Incident Angle ϕ

Same as the comparison between simulated result and experimental result we did in chapter 5.3 with theta angle, the phi angle is also under tested with its value from 0 degree to 30 degrees. The experimental results for absorptivity in different phi angles are plotted in Fig14 below. As the conclusion we got from the simulated result, with the increasing of phi angle, the absorptivity level inside bandwidth decreases.

From Fig14 below, the tested absorptivity level is better than simulated ones. When phi is equal to 10 degrees, it has an average absorptivity as 90%. 75% absorptivity in average for 20 degrees of phi and about 55% of average absorptivity when phi angle increases to 30 degrees. Unlike the simulated result, the tested result in different phi angles don't have any variation in bandwidth values.

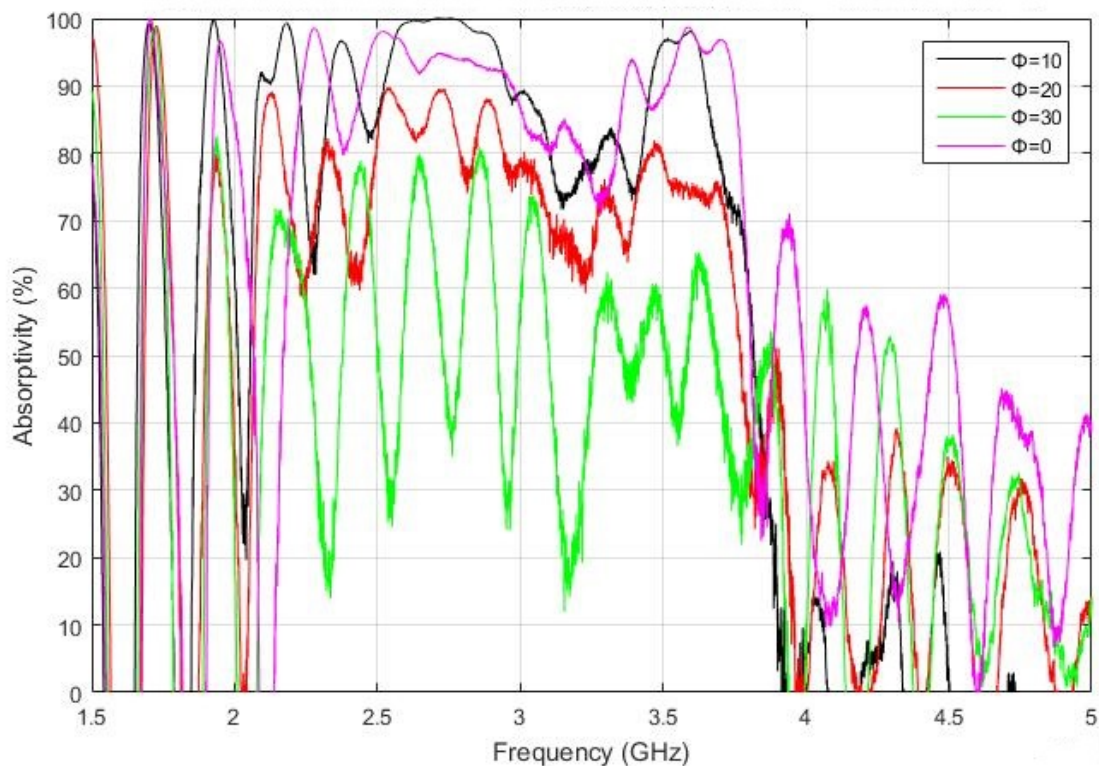


Figure 14 Absorptivity versus Frequency responses from polarization incident angle from 0 to 30 degree

6 Conclusion and future work

In this thesis project, a meta-material structured triple-layer absorber has been designed, constructed and manufactured, also the simulating and testing of it has been done and compared at the report. The triple-layer MMA consists seven layers, including four metallic films and three ISO680 substrate layers in between.

Simulated absorption bandwidth of the proposed structure is 1.85GHz from 2.25GHz to 4.1GHz, and the testing experimental results shows the fabricated MMA board has 1.5GHz bandwidth from 2.25GHz to 3.75GHz, where it starts at the same frequency but only have 80% of the entire designed bandwidth.

Furthermore, the sensitivities of structure were also studied under variations of dimensions, incident wave angles and polarization angles. With changing of scan angles theta and phi, the structure can keep its reliability until 50 degree of theta and 10 degree of phi.

The future work on this project should be focused on develop the reliability with fabricating and decrease the total thickness of the absorber as well.

References

- [1] Landy, N. I., Sajuyigbe, S., Mock, J., Smith, D. R., Padilla, W. J. 'A Perfect Metamaterial Absorber' 2008 *Phys. Rev. Lett* **99** 063908
- [2] Liu, R., Ji, C., Mock, J. J., et al. Broad ground-plan cloak [J]. *Science*, 2009, 323(5912): 366-369.
- [3] Zhou, Z., Huang, D., Liu, X., Mou, W., & Kang, F., (2014). Application Development of Metamaterials in Wideband Microwave Absorbing Materials. *Journal of materials engineering*. 1001-4381. 2014.05.016.
- [4] Claire M. Watts, Xianliang Liu, Wille J. Padilla. (2012). Metamaterial Electromagnetic Wave Absorbers. *Advanced Optical Materials*. *Adv. Mater.* 2012, 24, OP98-OP120.
- [5] S. Bhattacharyya et al. 'A Broadband Wide Angle Metamaterial Absorber for Defense Applications' *IEEE International Microwave and RF Conference*. Bangalore (India), December 2014.
- [6] Tao, H., Bingham, C., Pilon, D., Fan, K., Strikwerda, A., Shrekenhamer, D., Averitt, R. (2010). A dual band terahertz metamaterial absorber. *Journal of Physics D: Applied Physics* *J. Phys. D: Appl. Phys.*, 225102-225102.
- [7] Luo, H., Wang, T., Gong, R., Nie, Y., & Wang, X. (2010). Extending the Bandwidth of Electric Ring Resonator Metamaterial Absorber. *Chinese Physics Letters* *Chinese Phys. Lett.*, 034204-034204.
- [8] Sun, J., Liu, L., Dong, G., & Zhou, J. (2011). An extremely broad band metamaterial absorber based on destructive interference. *Opt. Express* *Optics Express*, 21155-21155.
- [9] Zhou Z., Huang D., Liu X., Mou W., & Kang F., (2014). Application Developments of Metamaterials in Wideband Microwave Absorbing Materials. 10.11868/j.issn.1001-4381. 2014.05.016.
- [10] David M. Pozar (u.d.), *Microwave Engineering*, 4th ed. p.cm. 2011033196, John Wiley & Sons, Inc. Page 16.

[11] Li M., Liu M., HFSS Electromagnetic Simulation Design., (2013). Posts & Telecom Press., 0441.4-39,. 220873. Page 80 -81.

[12] Wikipedia page, 'Printed circuit board', https://en.wikipedia.org/wiki/Printed_circuit_board.